Magnetic interactions in the metallic phase of the copper oxides: A Fermi-liquid description

Qimiao Si,* Jian Ping Lu,† and K. Levin
Department of Physics and the James Franck Institute, The University of Chicago, Chicago, Illinois 60637
(Received 26 November 1990)

One of the central issues in the field of high-temperature superconductivity is whether the normal state can be described by Fermi-liquid theory. Recent photoemission experiments along with a growing body of Fermi-liquid-based theoretical work have provided some support for this viewpoint. However, one major concern in ascertaining the validity of a Fermi-liquid approach is whether the magnetic interactions in the metallic cuprates are sufficiently strong so as to undermine the usual Fermi-liquid description. In this paper we address this question by examining the nature of the magnetic interactions in the metallic state. These interactions, which are dominantly between the Cu spins, arise via the intermediating oxygenlike states. Since the oxygen character changes as the hole doping is increased, it is expected that the Cu-Cu interactions are doping sensitive and evolve away from their value in the insulating limit. We deduce these interactions within a physical picture in which the Cu d electrons are nearly localized and the oxygen bandwidth assumes a finite value. While our qualitative results are general, we use a $1/N$ expansion as a convenient theoretical tool. In the extended Hubbard Hamiltonian the exchange terms are evaluated at order $(1/N^2)$. Both superexchange (J_S) and Ruderman-Kittel-Kasuya-Yosida interactions (J_R) emerge on a similar footing. With increasing carrier concentration, J_S decreases rapidly, while J_R abruptly increases from zero. We find that, because of the reduction in the strength of the superexchange, there is an enhanced stability of the Fermi-liquid phase. The dynamical susceptibility is also calculated within this scheme and the consequences for NMR and neutron experiments are discussed elsewhere.

I. INTRODUCTION

The nature of the magnetic interactions in the metallic state of the copper oxides and the associated dynamical susceptibility $\chi(q,\omega)$ are of central interest both to the superconducting as well as the normal-state properties. A quantitative understanding of the spin dynamics has been achieved for the half-filled insulating limit.[1] Here the Cu spins are localized and interact through oxygen sites via a superexchange interaction. Away from half-filling, the situation is less clear and the character and importance of spin fluctuation effects in the metallic phase have not been unambiguously established, in part because of problems with sample quality and ill-controlled oxygen stoichiometry.[2] Nevertheless there are features of these materials which we regard as noncontroversial. A growing body of evidence for the existence of a Fermi surface[3] implies that a Fermi-liquid description must be taken seriously at this stage. This picture must, on the other hand, be compatible with the observation that the copper electrons seem to behave as local or quasilocal moments, somewhat independent of carrier concentration.[4,5] In addition, magnetic order rapidly disappears before the onset of the metallic state. This suggests that it is the effective interactions rather than the moments which are modified with doping. On this basis we are motivated to study the behavior of the exchange interactions with varying carrier concentration using a Fermi-liquid description in which the Cu electrons are nearly but not completely localized. The related dynamical susceptibility which is essential for understanding neutron and NMR experiments is then deduced and the consequences for experiment discussed elsewhere.[6]

The standard argument that the Fermi-liquid phase is less stable than other more exotic magnetically driven phases is based, in part, on the assumption that the magnetic interactions in the metallic state are the same as their insulating counterparts. However, these magnetic interactions are mediated by oxygen sites (and spins) whose character is changing as the insulator evolves into a metal. It is therefore essential to reexamine the Cu-Cu exchange interactions in the context of variable hole concentration. Our conclusions here are that a rapid suppression of the superexchange in conjunction with a growth of the Ruderman-Kittel-Kasuya-Yosida (RKKY) interaction reinforce the stability of a Fermi-liquid phase. These results are demonstrated in the context of a mean-field phase-diagram calculation. Further evidence for a Fermi-liquid-based scheme, as well as a general discussion of transport and magnetic "anomalies" in the cuprates, is reviewed in Ref. 7.

The rest of the paper is organized as follows. In Sec. II we discuss our model and formalism for deriving the exchange interactions. The doping concentration dependence of the derived exchange interactions is analyzed in Sec. III. Section IV is devoted to a discussion of the RPA dynamical spin susceptibility. In Sec. V the competition between the Fermi-liquid phase and various magnetic phases is examined. Section VI presents our conclusions. The details of the calculations are presented in three appendixes. This organization should make it easier for the reader uninterested in the complex formalism to follow the body of the paper.

II. THEORETICAL FRAMEWORK

We calculate the magnetic interactions using the quasiparticle vertex function. This approach is more direct

than previous energy-based schemes applied at half-filling.[8] Our starting point is the usual extended Hubbard Hamiltonian in the auxiliary boson scheme[7,9,10] which has also been widely applied to heavy fermions.[11,12] We stress here that at the qualitative level, our results for the strength of the spin-spin interaction can be viewed as general consequences of the three-band Hamiltonian with very strong Coulomb correlations U. Here, for definiteness we use a controlled $1/N$ (where N is the spin degeneracy) expansion which is the basis for a mean-field theory and its RPA extension. The CuO_2 Hamiltonian written in the auxiliary boson representation (with hole-state fermion operators) is given by

$$H=\sum_{i,\sigma}\varepsilon_d^0 d_{i\sigma}^\dagger d_{i\sigma}+\sum_{l,\sigma}\varepsilon_p p_{l\sigma}^\dagger p_{l\sigma}+\sum_{l_1,l_2,\sigma} t_{pp}(p_{l_1\sigma}^\dagger p_{l_2\sigma}+\text{H.c.})+\sum_i \varepsilon_e e_i^\dagger e_i+\sum_i \varepsilon_f f_i^\dagger f_i$$
$$+\sum_{i,l,\sigma} V_{pd}[e_i d_{i\sigma}^\dagger p_{l\sigma}+f_i^\dagger d_{i-\sigma}p_{l\sigma}\,\mathrm{sgn}(\sigma)+\text{H.c.}]+\sum_i i\lambda_i\left[\sum_\sigma d_{i\sigma}^\dagger d_{i\sigma}+e_i^\dagger e_i+f_i^\dagger f_i-NQ_0\right]. \quad (2.1)$$

Here we define $e_i^\dagger$, $d_{i\sigma}^\dagger$, and $f_i^\dagger$ as creation operators for the Cu^+, Cu^{2+}, and Cu^{3+} valence states, respectively. The first and last of these correspond to bosons whereas the Cu^{2+} state is a fermion with specified spin index σ. This Hamiltonian is derived from the extended Hubbard Hamiltonian by representing a copper electron operator in terms of its valence state operators as $D_{i\sigma}^\dagger=d_{i\sigma}^\dagger e_i+\mathrm{sgn}\sigma\, d_{i-\sigma}f_i^\dagger$. The energy to create a Cu^+ (no hole) state is $\varepsilon_e=0$, and that to create a Cu^{3+} state (two holes) is $\varepsilon_f=2\varepsilon_d^0+U$. In Eq. (2.1) a Lagrange multiplier $i\lambda_i$ is introduced to account for all possible valence states at each Cu site so that

$$\sum_\sigma d_{i\sigma}^\dagger d_{i\sigma}+e_i^\dagger e_i+f_i^\dagger f_i=1=NQ_0\ . \quad (2.2)$$

In the context of a controlled $1/N$ expansion, we choose $Q_0=1/N$ to be finite, and V_{pd} is understood to be order $1/\sqrt{N}$.

The Hamiltonian thus includes copper-oxygen hybridization V_{pd}, a finite oxygen dispersion derived from t_{pp} [and called $\varepsilon(k)$] and oxygen and "bare" copper levels called ε_p and ε_d^0, respectively. The parameters appropriate to the copper oxides,[13] which we will use throughout this paper are such that all three valence states are probably admixed. However, it is often assumed that the d-d Coulomb repulsion U can be replaced by infinity so that one of the two valence states is absent: Cu^{3+} in the "hole" picture and Cu^+ in the "electron" picture. In this paper we will refer to the large-U hole picture, although our qualitative as well as some quantitative conclusions are more general. Throughout the body of our work[7] using this boson formalism we have attempted to discuss both pictures, so that all results can be seen as general.

Equation (2.1) is a useful starting point for applying a steepest-descent approximation within a path-integral formulation. This mean-field approximation is exact in the limit that the spin degeneracy of the Cu and oxygen spin states (N) is infinite. While in reality $N=2$ is not large, this approximation has been rather successful in the context of heavy fermions and is believed to be a useful theoretical tool for the copper oxides. Since at infinite U only the e boson is present, we may replace this boson and the constraint field by static uniform c-numbers. Only the amplitude of the boson field is relevant, as a result of a gauge transformation.[14] We define $\langle i\lambda_k\rangle=\lambda_0\delta_{k,0}$ and $\langle |e|_k\rangle=e_0\delta_{k,0}$, since spatial fluctuations are of higher order in N. In this leading-order limit, Eq. (2.1) reduces to a mean-field Hamiltonian, which can be diagonalized to yield the renormalized band structure $E_n(\mathbf{k})$

$$H^{mf}=\sum_{n=1}^{3}\sum_{\mathbf{k},\sigma}E_n(\mathbf{k})\Phi_{n\mathbf{k},\sigma}^\dagger\Phi_{n\mathbf{k},\sigma}+\lambda_0(e_0^2-NQ_0)\ . \quad (2.3)$$

The quasiparticles $\Phi_{n\mathbf{k},\sigma}$ are composites of the original p,d operators. We define $\Psi_1=p_x$, $\Psi_2=p_y$ and $\Psi_3=d_{x^2-y^2}$, so that

$$\Phi_{n\mathbf{k},\sigma}=\sum_{r=1}^{3}u_{nr}(\mathbf{k})\Psi_{r\mathbf{k}\sigma}\ , \quad (2.4)$$

where $u_{nr}(\mathbf{k})$ are the coherence factors. To obtain the complete mean-field solution, one determines the parameters e_0 and λ_0 variationally by minimizing the free energy.

In the hole picture, for sufficiently small hybridization (V_{pd} of order 1 eV) the system undergoes a Brinkman-Rice localization transition ($m^*\to\infty$) (Refs. 7 and 10) at half-filling in which the renormalized hybridization vanishes ($e_0V_{pd}\to 0$). This signals the breakdown of the Fermi liquid as the insulator is approached. We view this as an important restriction on any Fermi-liquid-based approach. In the "electron" picture this occurs without constraints on the Hamiltonian parametrization. A residual effect of this localization driven insulating behavior, is that in the metallic state the Cu d electrons are almost localized corresponding to a moderately large mass enhancement. This behavior is closely analogous to the band narrowing or kinetic-energy renormalization found in the large-U limit of the Hubbard model.

A schematic plot of this renormalized band structure is shown in the inset of Fig. 1a. Here we consider a simplified model in which the oxygen band has parabolic dispersion and the hybridization is a wave-vector-independent constant[9] V. We have also repeated this (and all other calculations throughout this paper) for the more appropriate, although more complex, tight-binding band structure of the oxides. As can be seen by comparison with Ref. 7, the resulting band structure is not significantly different from that derived in a tight-binding scheme. The lower band has dominantly Cu character with a bandwidth which vanishes as δ. An important energy scale in the renormalized band structure is the gap Δ

between the upper and the lower band, which is small compared to the unhybridized oxygen bandwidth[13] D.

In the $1/N$ scheme, spin-spin interactions enter[12] at the $(1/N)^2$ level, as shown in the inset of Fig. 1(a). Here the solid lines correspond to the quasiparticle propagators

$$G_n(\mathbf{k},\omega)=[\omega-E_n-\Sigma(\mathbf{k},\omega)]^{-1}\ , \tag{2.5}$$

where $\Sigma(\mathbf{k},\omega)$ is the self-energy of the quasiparticles. The dotted lines are the renormalized slave boson propagators associated with *fluctuations* in both the Cu^+ and Cu^{3+} bosons

$$D(\mathbf{k},\omega)=[D_0^{-1}+\Pi(\mathbf{k},\omega)]^{-1} \tag{2.6}$$

and $-\Pi(\mathbf{k},\omega)$ is the boson self-energy. At small frequencies ($\omega<\Delta$), there are strong renormalization effects. However, in the limit that $\Delta\ll D$, the dominant contribution to the exchange interactions arises from high-frequency fluctuations. The expressions for the relevant boson propagators are given in Appendix A, where the details of the exchange interaction calculation are also presented. At high frequencies, the quasiparticles are dominantly of p character. At low frequencies, on the other hand, the quasiparticles on the external legs can be replaced by copper states at the Fermi energy. As a result, the final expressions for the exchange interactions can be decomposed in the following two contributions:

$$J_R(R_{ij})=4V^4\int\frac{d\mathbf{k}_1}{\Omega}\frac{d\mathbf{k}_2}{\Omega}e^{i(\mathbf{k}_1-\mathbf{k}_2)\cdot\mathbf{R}_{ij}}f^-_{\mathbf{k}_1}f^+_{\mathbf{k}_2}\left[\left[\frac{1}{\varepsilon_{\mathbf{k}_2 d}}+\frac{1}{\varepsilon_{u\mathbf{k}_1}}\right]^2\frac{1}{\varepsilon_{\mathbf{k}_1}-\varepsilon_{\mathbf{k}_2}}-\frac{2}{U\varepsilon_{\mathbf{k}_2 d}\varepsilon_{u\mathbf{k}_1}}\right] \tag{2.7a}$$

and

$$J_S(R_{ij})=4V^4\int\frac{d\mathbf{k}_1}{\Omega}\frac{d\mathbf{k}_2}{\Omega}e^{i(\mathbf{k}_1-\mathbf{k}_2)\cdot\mathbf{R}_{ij}}\left[\left[\frac{1}{\varepsilon_{\mathbf{k}_1 d}}+\frac{1}{U}\right]\frac{f^+_{\mathbf{k}_1}f^+_{\mathbf{k}_2}}{\varepsilon_{\mathbf{k}_1 d}\varepsilon_{\mathbf{k}_2 d}}+\left[\frac{1}{\varepsilon_{u\mathbf{k}_1}}+\frac{1}{U}\right]\frac{f^-_{\mathbf{k}_1}f^-_{\mathbf{k}_2}}{\varepsilon_{u\mathbf{k}_1}\varepsilon_{u\mathbf{k}_2}}\right]\ , \tag{2.7b}$$

where $\varepsilon_{\mathbf{k}d}=(\varepsilon_{\mathbf{k}}-\varepsilon_d^0)$, $\varepsilon_{u\mathbf{k}}=(U+\varepsilon_d^0-\varepsilon_{\mathbf{k}})$, Ω is the volume of the Brillouin zone, $f^-_{\mathbf{k}}$ is the Fermi function and $f^+_{\mathbf{k}}=(1-f^-_{\mathbf{k}})$.

These terms arise from poles in both the fermion and the boson propagators. Because of the combination of Fermi functions involved in these expressions, J_R can be identified with the RKKY interaction and J_S with the "superexchange" term. It should be stressed that it is their sum J_H, which is physically relevant. Nevertheless we make this separation on the basis of a perturbative calculation of the exchange interactions, which is given in Appendix B. Physically the RKKY term[15] may be thought of as deriving from an intermediate oxygen state, which contains a hole and therefore a spin, whereas the (infinite-U) superexchange term arises when the intermediate oxygen state is empty of holes. Clearly, as excess holes populate the bare oxygen band the relative importance of these two terms changes.

III. CONCENTRATION DEPENDENCE OF EXCHANGE INTERACTIONS

To find the concentration dependence of these interactions we have numerically evaluated the two contributions in Eqs. (2.7). In the isotropic model discussed above, the integrals in Eqs. (2.7) reduce to a one-dimensional limit. In the tight-binding scheme, more complex numerical calculations yield similar conclusions. In both cases we find that the range of the superexchange term increases as the oxygen band becomes broader, while that of the RKKY interaction is relatively less sensitive. Overall, the spatial dependence of the various interactions is oscillatory in sign. In Fig. 1(a), the nearest-neighbor interactions are plotted in units of $4V^4/(\varepsilon_p-\varepsilon_d^0)^3$ as a function of doping concentration δ. Here for definiteness we assume $U=\infty$ and $(\varepsilon_p-\varepsilon_d^0)=0.7D$. The figure illustrates how the RKKY interaction quickly sets in as the dopant concentration increases, while the superexchange term decays rapidly with increasing hole number. The sum of both contributions is indicated by J_H in the figure.

It can be seen that for a range of values of δ the next-nearest-neighbor exchange interaction is ferromagnetic in sign. The notion that there is a ferromagnetic frustration to the antiferromagnetic superexchange has been recognized in the literature both experimentally[4] and theoretically[15,16] within the context of a more localized description. Our numerical analysis pertains to the limit of arbitrarily small Δ/D. Estimates based on slightly larger and more physically appropriate values of this parameter ($\Delta/D=0.02$) yield the same qualitative behavior with a *reduced* RKKY term. Thus, we believe that the RKKY interaction is overestimated in Fig. 1, so that in the metallic regime, the dominant interaction may still be the antiferromagnetic superexchange coupling, with a significantly reduced magnitude.

In the half-filled-band limit ($\delta=0$), for zero oxygen bandwidth, our formalism yields the results of Ref. 17. (This analysis depends on the inclusion of various form factors associated with the CuO_2 tight-binding description.) Our theory, furthermore, provides a natural extension of the results of Ref. 17 to the more physically appropriate case of a large oxygen bandwidth. Results equivalent to the expressions in Eqs. (2.7) have been deduced by Gor'kov and Sokol[16] for a modified Fermi-liquid model with $U=\infty$ and in which the copper spins are fully localized. This represents a *qualitatively* different model from the hybridized Fermi liquid we discuss here; the similarity in the results of the final analysis can be attributed to our assumption that $D\gg\Delta$. The above discussion underlines the fact that the present results are insensitive (at the general physical level) to the

details of the auxiliary boson scheme. We may, thus, view our calculations as providing a reasonable interpolation scheme between the dilute and concentrated (i.e., Fermi-liquid) regimes, although they clearly do not include the complex physics associated with polaronic[15,16,18] or other more localized descriptions of the oxygen hole motion when the hole concentration is small but nonzero.[19]

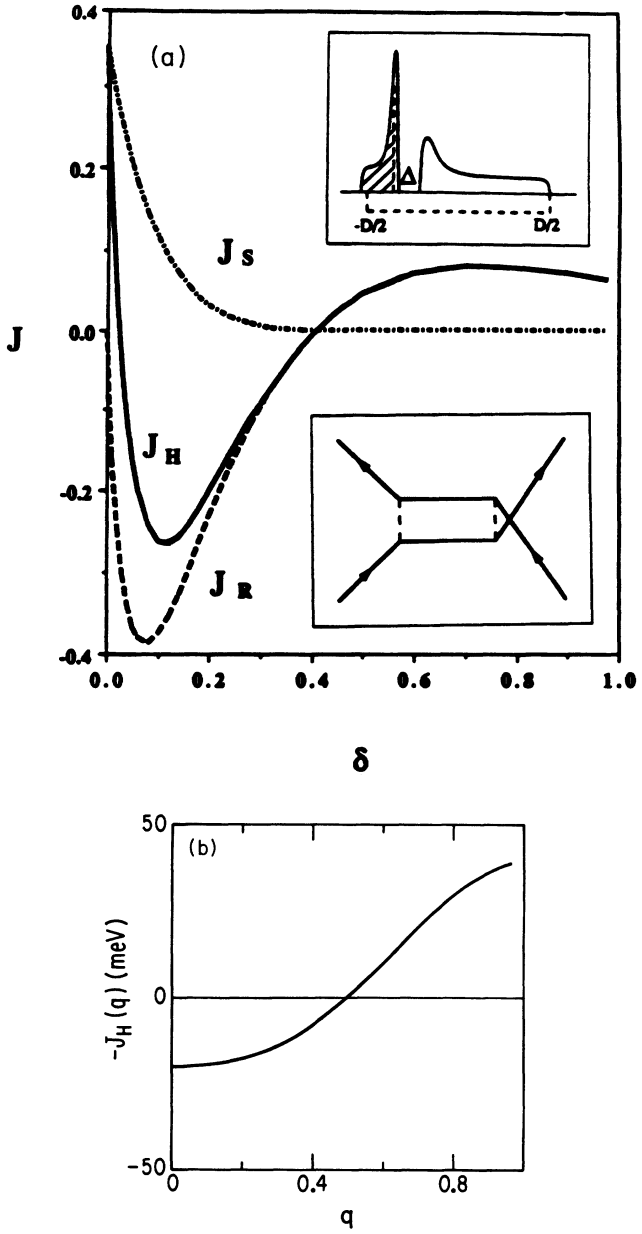

FIG. 1. (a) Doping concentration dependence of microscopically determined nearest-neighbor exchange interactions [in units of $4V^4/(\varepsilon_p-\varepsilon_d^0)^3$]: J_S, J_R, and J_H correspond to superexchange, RKKY and their total, respectively. In the insets are plotted the renormalized copper oxide band structure and $(1/N)^2$ exchange diagram. A parabolic oxygen band structure is assumed, for simplicity. (b) Exchange interaction J_H as a function of q at $x=0.04$ (in the tight-binding copper oxide model).

IV. CALCULATION OF THE DYNAMICAL SUSCEPTIBILITY

An RPA resummation of the dynamical susceptibility is not always possible, except for the case of constant J. However, because of the special structure of the vertex function in the present theory ($[J_H(q,\omega)/2]d^\dagger_{k+q\sigma}d^\dagger_{k'-q\sigma'}d_{k'\sigma}d_{k\sigma'}$), the RPA series can be summed to yield the dynamical susceptibility $\chi_{rr'}(q,\omega)$. The details are presented in Appendix C. Similar results are obtained in Ref. 20 for the heavy-fermion problem. We find that

$$\chi^{-+}_{rr'}=\chi^{0\,-+}_{rr'}(q,\omega)+\frac{\chi^{0\,-+}_{rd}(q,\omega)[-J_H(q)]\chi^{0\,-+}_{dr'}(q,\omega)}{1+J_H(q)\chi^{0\,-+}_{dd}(q,\omega)} \tag{4.1}$$

where $\chi^0_{rr'}(q,\omega)$ is the Lindhard susceptibility associated with the *renormalized* band structure and the subscript r corresponds to oxygen (p) or Cu (d) states. Equation (4.1) contains the essential physics of our Fermi-liquid description of the magnetic properties. Its general form coincides with that *assumed* in Ref. 21.

There are two important ingredients to the dynamical susceptibility of Eq. (4.1). These are (1) the band structure renormalizations contained in χ^0 and (2) the quasiparticle exchange interactions, J_H. These two components are characteristic of any Landau Fermi-liquid picture. Indeed the static uniform susceptibility of Landau theory consists of m^*/m and F_0^a contributions, which play a similar role at $q=0$ to our two finite q contributions. In general, these two cannot be clearly separated, using only magnetic measurements. In our strongly correlated system, the quasiparticle bandwidth is considerably more narrow than in a noninteracting system. This introduces a new energy scale which appears in χ^0. This reduction in bandwidth is associated in an essential way with the "quasilocalization" of the d electrons which forms the basis for our physical picture. It is clear that nesting effects, which lead to q-dependent contributions, as well as structure associated with Van Hove singularities will be accentuated in this narrow band limit. These may show up as "antiferromagnetic" structure, although in reality they are not associated with the exchange interactions. It is natural, then, to view the magnetism as a strongly combined effect of band structure and interactions. The two extreme limits of this picture yield the "nearly magnetic" approaches of Ref. 21 and the "nearly localized" approach of the present paper. In reality, a more realistic situation may lie somewhere in between. By tuning the size of the interaction term J_H, as well as other parameters, our microscopic approach can incorporate either physical picture. Which alternative is more appropriate is best determined phenomenologically by detailed comparison with a wide class of magnetic as well as transport data. This issue is discussed in more detail elsewhere.[6]

We end this section with a discussion of the q dependence of the exchange interaction $J_H(q)$. This function is an important input parameter for calculations of $\chi(q,\omega)$, which have been presented in Ref. 6. In order to lay the

groundwork for calculations of the spin dynamics in the cuprates, we consider the more realistic tight-binding description of the oxygen bands which is found to give results similar to those of the parabolic model. In Fig. 1(b) is plotted the net exchange interaction as a function of wave vector q for a doping concentration $x=0.04$, where the interaction is dominated by the antiferromagnetic superexchange. Here the insulating limit (100 meV) is fitted. It may be seen that this q dependence is roughly represented by a simple tight-binding $\cos q_{x,y}a$ form. It should be stressed that this form is only appropriate for the tight-binding description of the CuO_2 planes. While, Fig. 1(b) addresses a rather low x value (in order to exhibit results for a clearly antiferromagnetic exchange), we have verified that this q dependence is also appropriate for higher values of x. This q-dependent exchange is found to play an important role in the dynamical susceptibility, particularly in the $YBa_2Cu_3O_7$ system.[6] In the antiferromagnetic regime, it also has the effect of *suppressing* the magnitude of the Pauli term relative to the noninteracting quasiparticle limit.

V. IMPLICATIONS FOR THE PHASE DIAGRAM

To analyze the phase diagram we compare the energy of the Fermi-liquid state with that of various magnetic states. We derive the "Kondo-Heisenberg" Hamiltonian

$$H_{\rm eff}=\sum_{i,\sigma}\varepsilon_d^0 d_{i,\sigma}^\dagger d_{i\sigma}+\sum_{l,\sigma}\varepsilon_p p_{l,\sigma}^\dagger p_{l,\sigma}+\sum_{l_1,l_2,\sigma} t_{pp}(p_{l_1,\sigma}^\dagger p_{l_2,\sigma}+\text{H.c.})+\sum_i i\lambda_i\left[\sum_\sigma d_{i\sigma}^\dagger d_{i\sigma}-1\right],$$
$$+\sum_{i,l_1,l_2,\sigma,\sigma'}\tfrac{1}{2}J_K d_{i\sigma}^\dagger p_{l_1\sigma'}^\dagger p_{l_2\sigma} d_{i\sigma'}+\sum_{i,j,\sigma,\sigma'}\tfrac{1}{2}J_S(R_{ij}) d_{i\sigma}^\dagger d_{j\sigma'}^\dagger d_{j\sigma} d_{i\sigma'} \tag{5.1}$$

using a path-integral scheme applied directly to the extended Hubbard Hamiltonian by integrating out the Cu^+ and Cu^{3+} bosons and truncating after terms of order V^4. Written in this way the Schrieffer-Wolff or Kondo exchange interaction J_K which is formally of order V^2 will lead to the RKKY interaction of Eq. (2.7) when it is treated in second-order perturbation theory. The value of J_S deduced in this perturbative (in V) approach is found to be equivalent to the expression in Eq. (2.7), derived within the $1/N$ formalism. This scheme such as the diagrammatic approach yields specific values for the appropriate exchange constants which have been previously taken to be unconstrained.[22] The details of this analysis are sufficiently complex so that they are deferred to Appendix B.

The free energies of the Fermi-liquid (FL) and various *localized* magnetic phases are calculated using Eq. (5.1) within a mean-field approximation in which, for simplicity only the nearest-neighbor exchange interactions are included. We rewrite Eq. (5.1) using a Hubbard-Stratonovich bosonization scheme

$$H'_{\rm eff}=\sum_{i,\sigma}\varepsilon_d^0 d_{i\sigma}^\dagger d_{i\sigma}+\sum_{l,\sigma}\varepsilon_p p_{l\sigma}^\dagger p_{l\sigma}+\sum_{l,l',\sigma} t_{pp} p_{l\sigma}^\dagger p_{l'\sigma}+\sum_{i,\sigma} i\lambda_i(d_{i\sigma}^\dagger d_{i\sigma}-1)-\frac{1}{2}J_K\sum_{i,l\subset i,\sigma\neq\sigma'}[X_{i\sigma\sigma'}(d_{i\sigma}^\dagger p_{l\sigma}+p_{l\sigma'}^\dagger d_{i\sigma'})-\tfrac{1}{2}X_{i\sigma\sigma'}^2]$$
$$+\frac{1}{2}J_K\sum_{i,l\subset i,\sigma}(U_{i\sigma}d_{i\sigma}^\dagger d_{i\sigma}+V_{i\sigma}p_{l\sigma}^\dagger p_{l\sigma}-U_{i\sigma}V_{i\sigma})+\frac{1}{2}J_S\sum_{\langle ij\rangle,\sigma,\sigma'}(d_{i\sigma}^\dagger W_{j\sigma\sigma'}d_{i\sigma'}-\tfrac{1}{2}W_{i\sigma\sigma'}W_{j\sigma\sigma'}). \tag{5.2}$$

Here J_K is given by $2V^2/(\varepsilon_p-\varepsilon_d^0)$ and J_S is parametrized from Fig. 1 as $J_S(\delta)=[4V^4/(\varepsilon_p-\varepsilon_d^0)^3]\exp(-\delta/\delta_0)$. The various Hubbard-Stratonovich fields are defined as

$$X_{i\sigma\sigma'}=\sum_{l\subset i}p_{i\sigma'}^\dagger d_{i\sigma'},\quad U_{i\sigma}=\sum_{l\subset i}p_{l\sigma}^\dagger p_{l\sigma},$$
$$V_{i\sigma}=d_{i\sigma}^\dagger d_{i\sigma},\quad W_{i\sigma\sigma'}=d_{i\sigma'}d_{i\sigma}^\dagger. \tag{5.3}$$

Different choices of the mean-field ansatz for $\{X,U,V,W\}$ lead to different mean-field phases.

The mean-field phase diagram[23] resulting from this analysis is shown in Fig. 2. The shaded region indicates the physical parameter space, i.e., that which yields energy scales appropriate for the copper oxides. While the present analysis addresses a simple spherical band, we expect these results to be more general, since the phase diagram depends primarily on details of the energies, rather than on those of the band-structure parametrization. For comparison, in the inset we plot the corresponding phase diagram when the oxygen band is dispersionless and the superexchange interaction is a constant given by $J_S=4V_{pd}^4/(\varepsilon_p-\varepsilon_d^0)^3$. In this case, for the physical parameter space, magnetic order persists over a wider range of δ. This comparison thus illustrates how the doping concentration dependence of the exchange interactions enhances the stability of the Fermi-liquid phase.

Because of the oscillatory nature of the exchange interactions, which is not properly accounted for in our truncation scheme, the ferromagnetic (F) and antiferromagnetic (AF) phases, which are indicated in the lower half of the phase diagram, presumably have spiral order with a corresponding pitch, which evolves continuously from F-like to AF-like as the doping concentration is increased. Comparing Figs. 2 and 1, it may be seen that the mean-field phase boundaries between the AF and F phases mirror the sign changes found in the vertex function J_H. A full analysis, which treats various spin-liquid phases in the presence of a finite oxygen bandwidth, requires a new (Schwinger boson-slave fermion) formalism. However, it may be inferred from previous calculations in the t-J model[24] that a spin-liquid-like phase will occur somewhat near the boundary of the AF and FL states. The stability of this phase will be adversely affected by the growing tendency towards nearest-neighbor ferromagnetic fluctuations seen in Fig. 1. It should be stressed that, while, Eq. (5.1) contains the precise RKKY interaction [of Eq. (2.7a)], at the mean-field level only the uniform part of the spatially dependent RKKY interac-

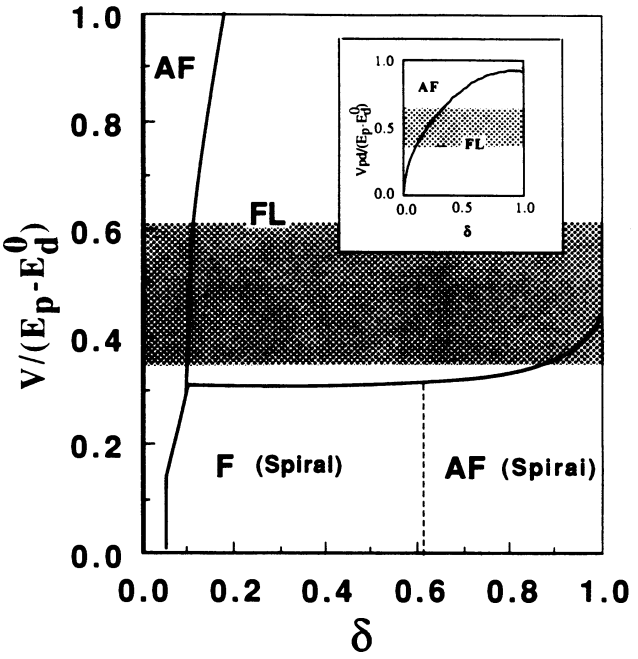

FIG. 2. The mean-field phase diagram for physically large conduction band width. In the inset is plotted the analogous phase diagram for zero bandwidth. F, AF, FL stand for ferromagnetic, antiferromagnetic, and Fermi-liquid phases, respectively. The shaded region corresponds to the physical parameter region (see text). The F and AF phases exhibit spiral order, as also discussed in the text.

tion is included. This underlines the pitfalls associated with deriving exchange interactions directly from mean-field energy considerations.

VI. CONCLUSIONS

In summary, this paper has presented a number of results: (1) We have addressed the nature of the exchange interactions in the metallic copper oxides and demonstrated that the character and magnitude of these interactions is sensitive to the hole concentration. In addition we have shown that it has considerable q structure and that to a good approximation, this q dependence can be approximated by a simple nearest-neighbor tight-binding form. This form is particularly important in explaining the spin dynamical properties of the Y-Ba-Cu-O family.[6] (2) We have presented a microscopically based calculation of the dynamical susceptibility of the Fermi-liquid phase. This susceptibility plays an important role in interpreting[6] NMR and neutron data and has in the past either been treated phenomenologically or assumed to be of the small Coulomb U, RPA form, with adjustable carrier concentration.[21] In our calculations the hole concentration is taken to be the physical value. Furthermore, we have performed these calculations for various three-band extended Hubbard models in which the oxygen band is treated as having a free-electron-like, as well as tight-binding dispersion. (3) Finally our self-consistently determined exchange interactions have been used to demonstrate the enhanced stability of the Fermi-liquid phase. This last point also bears on a large body of theoretical work based on the t-J model in which J is assumed to have the value appropriate to the insulator.

To what extent have the exchange interactions in the metallic phase been characterized experimentally? There is a significant body of evidence for little change in the character of the Cu states with doping.[4,5] This reinforces our "quasilocalized" Fermi-liquid picture and suggests that the rapid loss of magnetic order with additional holes may derive from the changes in the exchange interaction. Johnston has analyzed susceptibility data[25] and deduced a suppression in the exchange interaction with doping, although a number of uncontrolled assumptions have been made in this analysis. Neutron data have indicated that magnetic-induced structure and correlations are progressively more difficult to observe with increased hole doping.[26] Raman experiments have also been interpreted as suggesting that the exchange interaction is suppressed with increasing oxygen content.[27] The nature of the magnetic interactions will presumably become clearer shortly, but as yet there are no definitive answers.

What are the implications of the present work for Fermi-liquid theories? We have made two essential points relating to Fermi-liquid-based approaches. (1) The stability of the Fermi-liquid phase is enhanced by the suppression of the superexchange interactions found here. (2) Any interpretation of the experimentally measured dynamical susceptibility must recognize that band-structure renormalizations and the quasiparticle exchange interactions both enter into the analysis. These two contributions are difficult to separate and as a result, there may be "tradeoffs" between low-energy scales introduced by band-narrowing effects and by spin fluctuations. Our analysis,[7] thus far, has led us to conclude that the cuprates would be in a Fermi-liquid ground state, if superconductivity did not intervene. However, at the relatively "high" temperatures of the normal state there is a loss of full coherence so that transport and magnetic properties may exhibit anomalies. These are similar in many ways to those seen in the heavy-fermion metals at analogously high temperatures.[28]

ACKNOWLEDGMENTS

We thank Ju H. Kim for many helpful conversations. This work was supported by NSF-STC Grant No. STC-8809854 and NSF-MRL Grant No. 19860.

APPENDIX A: EVALUATION OF THE EXCHANGE INTERACTIONS WITHIN A $1/N$ FORMALISM

In this appendix, we derive the vertex function associated with the spin-spin exchange interactions between the *quasiparticles* of our Fermi liquid using a $1/N$ expansion. These interactions arise at the $(1/N)^2$ order. While the formalism is equivalent to that given in Ref. 12 for the heavy fermions, here we find a "superexchange" as well as an RKKY term. For definiteness, we work in the radial gauge.

Consider first the limit $U=\infty$. In the radial gauge the auxiliary boson field $(|e|,\lambda)$, where $|e|$ is the radial part of e field, can be decomposed into real and fluctuating parts:

$$|e|_k = e_0\delta_{k,0} + \sqrt{N}\,\delta r_k \ , \quad i\lambda_k = \lambda_0\delta_{k,0} + \delta\lambda_k \ , \tag{A1}$$

where e_0 and λ_0 are the variational parameters discussed in Sec. II. Here δr_k and $\delta\lambda_k$ are the fluctuating contributions which are integrated out. The exchange interactions arise from processes involving virtual quasiparticle states.

The auxiliary boson propagators are defined by

$$D(k,\tau) = \begin{bmatrix} D_{rr} & D_{r\lambda} \\ D_{\lambda r} & D_{\lambda\lambda} \end{bmatrix} = \begin{bmatrix} \langle T_\tau \delta r_k(\tau)\delta r_k(0)\rangle & \langle T_\tau \delta r_k(\tau)\delta\lambda_k(0)\rangle \\ \langle T_\tau \delta\lambda_k(\tau)\delta r_k(0)\rangle & \langle T_\tau \delta\lambda_k(\tau)\delta\lambda_k(0)\rangle \end{bmatrix} .$$

At high frequencies, the boson propagators on the lattice are essentially the same as for the impurity case, since all effects of p-d hybridization are irrelevant. Following Refs. 11 and 14, we find that at high frequencies,

$$D^{-1}(k,\omega) \approx \begin{bmatrix} N(-\varepsilon_d^0) & \sqrt{N}e_0 \\ \sqrt{N}e_0 & \dfrac{e_0^2(-\varepsilon_d^0)}{\omega^2} \end{bmatrix} . \tag{A2}$$

This leads to

$$D_{rr} \approx \frac{1}{2N}\left[\frac{1}{\omega-\varepsilon_d^0} + \frac{1}{-\omega-\varepsilon_d^0}\right] , \tag{A3a}$$

$$D_{r\lambda} = D_{\lambda r} \approx \frac{1}{2N}\frac{\sqrt{N}\,\omega}{e_0}\left[\frac{1}{\omega-\varepsilon_d^0} - \frac{1}{-\omega-\varepsilon_d^0}\right] , \tag{A3b}$$

$$D_{\lambda\lambda} \approx \frac{1}{2N}\left[\frac{\sqrt{N}\,\omega}{e_0}\right]^2\left[\frac{1}{\omega-\varepsilon_d^0} + \frac{1}{-\omega-\varepsilon_d^0}\right] . \tag{A3c}$$

The resulting propagators have poles at $\pm\varepsilon_d^0$, which reflect the charge transfer channel in the Hamiltonian. In the radial gauge, these poles occur only when the small $1/\omega^2$ diagonal element and an off-diagonal $\sqrt{N}e_0$ term are retained. These effects arise from preserving gauge invariance.

It may be seen from Eq. (A3) that the residues at these poles for D_{rr}, $D_{r\lambda}$, and $D_{\lambda\lambda}$ have the ratio $1:(\sqrt{N}\,\omega/e_0):(\sqrt{N}\,\omega/e_0)^2$, respectively. Thus, in the radial gauge, several different diagrams contribute at the same level to the vertex function. Each term can be associated with a different component of the matrix boson propagator, D_{rr}, $D_{r\lambda}$, or $D_{\lambda\lambda}$ inserted into the diagram given in Fig. 1. In each case the external legs can be approximated by the propagator for the d electrons at the Fermi level with intermediate fermion propagators determined by the corresponding interaction vertex. Each diagram has contributions from boson and fermion poles.

To express our results in final form, we use the following relations for $N=2$,

$$\sum_{\sigma,\sigma'} d_{i\sigma}^\dagger d_{j\sigma'}^\dagger d_{j\sigma} d_{i\sigma'} = 2(\mathbf{S}_i\cdot\mathbf{S}_j + \tfrac{1}{4}n_i n_j) \tag{A4a}$$

$$\sum_{\sigma,\sigma'} d_{i-\sigma}^\dagger d_{j\sigma}^\dagger d_{j\sigma'} d_{i-\sigma'}\,\mathrm{sgn}(\sigma\sigma') = 2(\mathbf{S}_i\cdot\mathbf{S}_j - \tfrac{1}{4}n_i n_j) \tag{A4b}$$

The resulting expressions for the exchange interactions can be separated into two parts.

$$J_S^{ee}(R_{ij}) = 4V^4\int \frac{D\mathbf{k}}{\Omega}\frac{D\mathbf{k}}{\Omega}\frac{f^+(\varepsilon_k)f^+(\varepsilon_{k'})}{(\varepsilon_k-\varepsilon_d^0)^2(\varepsilon_{k'}-\varepsilon_d^0)} \times e^{i(\mathbf{k}'-\mathbf{k})\cdot\mathbf{R}_{ij}} \tag{A5a}$$

and

$$J_R^{ee}(R_{ij}) = 4V^4\int \frac{D\mathbf{k}}{\Omega}\frac{D\mathbf{k}}{\Omega}\frac{f^+(\varepsilon_k)f^-(\varepsilon_{k'})}{(\varepsilon_k-\varepsilon_d^0)^2(\varepsilon_{k'}-\varepsilon_k)} \times e^{i(\mathbf{k}'-\mathbf{k})\cdot\mathbf{R}_{ij}} . \tag{A5b}$$

From the combination of the various Fermi functions we can identify J_S with the superexchange interaction and J_R with the RKKY interaction.

We now discuss *finite* but *large* U so that $\langle f\rangle = 0$ is preserved and $\delta f = f$ fluctuations will not give rise to infrared divergences. We use auxiliary boson fields $(\delta r, \delta\lambda, \delta f, \delta f^\dagger)$. The effect of finite U is to produce a similar propagator for the δf field with a pole at $(U+\varepsilon_d^0)$. This reflects the Mott-Hubbard channel. Calculating the diagrams with δf propagators we find that the resulting contribution to the exchange interactions can be separated into

$$J_S^{ff}(R_{ij}) = 4V^4\int \frac{D\mathbf{k}}{\Omega}\frac{D\mathbf{k}}{\Omega}\frac{f^-(\varepsilon_k)f^-(\varepsilon_{k'})}{(U+\varepsilon_d^0-\varepsilon_k)^2(U+\varepsilon_d^0-\varepsilon_{k'})} \times e^{i(\mathbf{k}'-\mathbf{k})\cdot\mathbf{R}_{ij}} \tag{A6a}$$

and

$$J_R^{ff}(R_{ij}) = 4V^4\int \frac{D\mathbf{k}}{\Omega}\frac{D\mathbf{k}}{\Omega}\frac{f^-(\varepsilon_k)f^+(\varepsilon_{k'})}{(U+\varepsilon_d^0-\varepsilon_k)^2(\varepsilon_k-\varepsilon_{k'})} \times e^{i(\mathbf{k}'-\mathbf{k})\cdot\mathbf{R}_{ij}} . \tag{A6b}$$

Finally incorporating the cross terms, by using Eq. (A4b), yields

$$J_S^{ef}(R_{ij}) = 4V^4\int \frac{D\mathbf{k}}{\Omega}\frac{D\mathbf{k}'}{\Omega} \times \left[\frac{f^+(\varepsilon_k)f^+(\varepsilon_{k'})}{(\varepsilon_k-\varepsilon_d^0)(\varepsilon_{k'}-\varepsilon_d^0)} + \frac{f^-(\varepsilon_k)f^-(\varepsilon_{k'})}{(U+\varepsilon_d^0-\varepsilon_k)(U+\varepsilon_d^0-\varepsilon_{k'})}\right]\frac{1}{U} \tag{A7a}$$

and

$$J_R^{ef}(R_{ij}) = 4V^4\int \frac{D\mathbf{k}}{\Omega}\frac{D\mathbf{k}'}{\Omega}\frac{2f^-(\varepsilon_k)f^+(\varepsilon_{k'})}{(U+\varepsilon_d^0-\varepsilon_k)(\varepsilon_{k'}-\varepsilon_d^0)} \times \left[\frac{1}{(\varepsilon_k-\varepsilon_{k'})} - \frac{1}{U}\right] . \tag{A7b}$$

Collecting all terms in Eqs. (A5)–(A7), we find Eqs. (2.7) in the text.

APPENDIX B: PERTURBATIVE CALCULATION OF THE EXCHANGE INTERACTIONS

This appendix is devoted to an alternative derivation of exchange interactions using a perturbative formalism. Here it is assumed that V_{pd} [and more specifically $V_{pd}/(\varepsilon_p-\varepsilon_d^0)$ and $V_{pd}/(U+\varepsilon_d^0-\varepsilon_p)$] are small parameters. For simplicity, we assume the ground state consists of two components: conduction (p) electrons moving in the local moment (d) electron background. In this case $e_0=0$, and hence both the e and f fields represent fluctuation contributions which can be fully integrated out.

After this integration, the partition function is given by

$$Z=\int Dd\, D\bar{d}\, Dp\, D\bar{p}\exp\left[-\int_0^\beta D\tau L_{\text{eff}}\right], \tag{B1a}$$

where $\beta=1/T$. Here the temperature T is taken to be 0. L_{eff} is defined by

$$\exp\left[-\int_0^\beta D\tau L_{\text{eff}}\right]=\int De\, D\bar{e}\, Df\, D\bar{f} \times\exp\left[-\int_0^\beta D\tau L\right]. \tag{B1b}$$

This leads to

$$L_{\text{eff}}(\tau)=\sum_{i,\sigma}\bar{d}_{i\sigma}(\partial_\tau+\varepsilon_d)d_{i\sigma}+\sum_{k,\sigma}\bar{p}_{k\sigma}(\partial_\tau+\varepsilon_k)p_{k\sigma}+\sum_i\sum_{k,\sigma k',\sigma'}(\bar{d}_{i\sigma}p_{k\sigma}V_{ik}e^{-i\mathbf{k}\cdot\mathbf{R}i})G_e(\tau-\tau')(\bar{p}_{k'\sigma'}d_{i\sigma'}V_{ik'}e^{i\mathbf{k}'\cdot\mathbf{R}_i}) +\sum_i\sum_{k,\sigma k',\sigma'}[\bar{d}_{i\sigma}\bar{p}_{k-\sigma}V_{ik}\,\mathrm{sgn}(\sigma)e^{i\mathbf{k}\cdot\mathbf{R}i}]G_f(\tau-\tau')[p_{k'-\sigma'}d_{i\sigma'}V_{ik'}\,\mathrm{sgn}(\sigma')e^{-i\mathbf{k}'\cdot\mathbf{R}i}]\,. \tag{B2}$$

In the above equation G_a with $a=(e$ or $f)$ is the corresponding propagator which, at $T\to0$ is given by

$$G_a(\tau-\tau')=(\partial_\tau+\varepsilon_a+i\lambda)^{-1}_{\tau\tau'} =\theta(\tau-\tau')\exp[-(\varepsilon_a+i\lambda)(\tau-\tau')]\,, \tag{B3}$$

where $\varepsilon_f=2\varepsilon_d^0+U$. Here the energy levels are defined relative to the chemical potential, and $\theta(x)$ is the step function.

We further integrate out the virtual oxygen processes to calculate the exchange interactions between d spins.

$$Z=\int Dd\, D\bar{d}\exp(-S_{\text{eff}})\,. \tag{B4}$$

From Eqs. (B1) and (B2), one can see that S_{eff} may be expressed by fermion matrices:

$$S_{\text{eff}}=S_0+\mathrm{Tr}\ln(M_p+M_e+M_f) \tag{B5}$$

with

$$(M_p)_{k\sigma\tau,k'\sigma'\tau'}=(\partial_\tau+\varepsilon_k)_{\tau\tau'}\delta_{\sigma\sigma'}\delta_{kk'}\,, \tag{B6a}$$

$$(M_e)_{k\sigma\tau,k'\sigma'\tau'}=\int D\tau' V_{ik}V_{ik'}e^{i(\mathbf{k}'-\mathbf{k})\cdot\mathbf{R}i}d_{i\sigma'}(\tau) \times\tilde{G}_e(\tau-\tau')\bar{d}_{i\sigma}(\tau')\,, \tag{B6b}$$

$$(M_f)_{k\sigma\tau,k'\sigma'\tau'}=\int D\tau' V_{ik}V_{ik'}e^{i(\mathbf{k}'-\mathbf{k})\cdot\mathbf{R}_i}\bar{d}_{i-\sigma}(\tau) \times G_f(\tau-\tau')d_{i-\sigma'}(\tau')\,. \tag{B6c}$$

When deriving Eq. (B5) from Eqs. (B1)–(B4), we have interchanged τ and τ' in M_e, and thus in Eq. (B6b)

$$\tilde{G}_e(\tau-\tau')=\theta(\tau'-\tau)\exp[\varepsilon_e(\tau-\tau')]\,.$$

The matrices inside the logarithm may be separated into bare oxygen and fluctuating parts,

$$\mathrm{Tr}\ln(M_p+M_e+M_f)=\mathrm{Tr}\ln M_p+(\text{one-body terms}) -\tfrac{1}{2}\mathrm{Tr}(M_p^{-1}M_eM_p^{-1}M_e+2M_p^{-1}M_eM_p^{-1}M_e+M_p^{-1}M_fM_p^{-1}M_f)+(\text{higher-order terms}) \tag{B7}$$

The second-order terms in the expansion give the two body interactions between the copper electrons. Here the p electron propagator is given by

$$(M_p^{-1})_{k\tau\sigma,k\tau'\sigma}=(\partial_\tau+\varepsilon_{k\sigma}-\mu)^{-1}_{\tau\tau'} =\exp[-\varepsilon_{k\sigma}(\tau-\tau')][\theta(\tau-\tau')(1-n_{k\sigma})-\theta(\tau'-\tau)n_{k\sigma})]\,, \tag{B8}$$

which can be separated into a "particle" part

$$A_p=\exp[-\varepsilon_{k\sigma}(\tau-\tau')]\theta(\tau-\tau')(1-n_{k\sigma}) \tag{B8'a}$$

and a "hole" part

$$B_p=-\exp[-\varepsilon_{k\sigma}(\tau-\tau')]\theta(\tau'-\tau)n_{k\sigma}\,. \tag{B8'b}$$

Taking care of the subtle time ordering in manipulating the trace, we find that

$$-\tfrac{1}{2}\mathrm{Tr}(M_p^{-1}M_eM_p^{-1}M_e)=\bar{\sum_{i,j}}\sum_{\omega_1,\omega_2,\omega_3,\omega_4}\delta(\omega_1-\omega_1+\omega_3-\omega_4)\tfrac{1}{4}J^{ee}(\omega_1,\omega_2,\omega_3,\omega_4)\sum_{\sigma,\sigma'}\bar{d}_{i\sigma}(\omega_1)\bar{d}_{j\sigma'}(\omega_3)d_{j\sigma}(\omega_4)d_{i\sigma'}(\omega_2)\,, \tag{B9a}$$

$$-\mathrm{Tr}(M_p^{-1}M_eM_p^{-1}M_e)=\bar{\sum_{i,j}}\sum_{\omega_1,\omega_2,\omega_3,\omega_4}\delta(\omega_1-\omega_2+\omega_3-\omega_4)\tfrac{1}{4}J^{ef}(\omega_1,\omega_2,\omega_3,\omega_4)$$
$$\times\sum_{\sigma,\sigma'}\bar{d}_{i-\sigma}(\omega_1)\bar{d}_{j\sigma}(\omega_3)d_{j\sigma'}(\omega_4)d_{i-\sigma'}(\omega_2)\,\mathrm{sgn}(\sigma\sigma')\ , \tag{B9b}$$

and

$$-\tfrac{1}{2}\mathrm{Tr}(M_p^{-1}M_fM_p^{-1}M_f)=\bar{\sum_{i,j}}\sum_{\omega_1,\omega_2,\omega_3,\omega_4}\delta(\omega_1-\omega_2+\omega_3-\omega_4)\tfrac{1}{4}J^{ff}(\omega_1,\omega_1,\omega_3,\omega_4)\sum_{\sigma,\sigma'}\bar{d}_{i\sigma}(\omega_1)\bar{d}_{j\sigma'}(\omega_3)d_{j\sigma}(\omega_4)d_{i\sigma'}(\omega_2)\ , \tag{B9c}$$

where $\bar{\sum}_{i,j}$ represents the summation over i and j independently. When we convert to $\sum_{i,j}$, which sums a pair of (i,j) only once, a factor of 2 is produced. Relations similar to Eqs. (A4), but "off shell," can also be derived. We interpret the resulting expressions as operator relations so that J^{ab} in the above equations with $a,b=(e$ or $f)$ represent spin-spin interactions. The expressions for $J^{ab}(\omega_1,\omega_2,\omega_3,\omega_4)$ for general $\omega_1,\omega_2,\omega_3,\omega_4$ are too complex to write down. However, in the "on-shell" limit, i.e., $\omega_1=\omega_2=\omega_3=\omega_4=i\lambda+\varepsilon_d^0$, we find that the part of J^{ab} which arises from $\mathrm{Tr}(AM_aAM_b)$ and $\mathrm{Tr}(BM_aBM_b)$ terms reduces to J_S^{ab} given in Eqs. (A5a), (A6a), and (A7a), while the part which comes from $\mathrm{Tr}(AM_aBM_b)$-like terms yields J_R^{ab} given in Eqs. (A5b), (A6b), and (A7b). (Here V^4 should be replaced by $V_{ij}V_{jk}V_{ik'}V_{jk'}$.)

In summary, this perturbative calculation gives results which are essentially equivalent to those derived in the $(1/N)$ expansion (in the small Δ/D limit) discussed in Appendix A.

APPENDIX C: RPA EVALUATION OF THE DYNAMICAL SPIN SUSCEPTIBILITY

In general only q-independent interactions have been shown[29] to be resummable within an RPA scheme. In the following we demonstrate that for the special combination of spin-spin and charge-charge interaction vertices Γ, which we find here

$$\Gamma\sim\sum_{i,j}J(R_{ij})(\mathbf{S}_i\cdot\mathbf{S}_j+\tfrac{1}{4}n_in_j)\ , \tag{C1}$$

the generalized *spin* susceptibility is resummable.

To set the stage for applications to magnetic experiments, we consider here a realistic tight-binding band structure appropriate to the copper oxide plane. The exchange interactions of Appendixes A and B are of the form $(\mathbf{S}\cdot\mathbf{S}+\frac{1}{4}nn)$ for the $U=\infty$ contribution, and $(\mathbf{S}\cdot\mathbf{S}-\frac{1}{4}nn)$ for the U-dependent contributions. In the present case where Coulomb correlations are strong, so that charge fluctuations are suppressed, we neglect the small differences between the structure of the vertices. We consider the general vertex function of Eq. (C1). Within this physical picture, the spin-spin interactions dominantly arise between the d components of the quasiparticles.

We start from the following effective Hamiltonian:

$$H_{\mathrm{eff}}=\sum_{n,k,\sigma}E_{nk\sigma}\Phi^{\dagger}{}_{nk\sigma}\Phi_{nk\sigma}$$
$$+\tfrac{1}{2}\sum_{K,k,k'\sigma,\sigma'}J_H(K)d^{\dagger}{}_{k+K\sigma}d^{\dagger}{}_{k'-K\sigma'}d_{k'\sigma}d_{k\sigma'}\ . \tag{C2}$$

Here the quasiparticle operators, $\Phi_{nk\sigma}$, are related to the wave functions, $\Psi_{rk\sigma}$, via coherence factors, u_{nr}, defined in Eq. (2.4). We use the equation of motion method and follow the notation of Ref. 30.

We first introduce dynamical susceptibilities associated with the different components by

$$\chi^{-+}_{rr'}(q,t)=i\theta(t)\langle[\sigma^-_r(q,t),\sigma^+_{r'}(0,0)]\rangle\ , \tag{C3}$$

where σ^- and σ^+ are the spin lowering and raising operators. We also define

$$\chi^{-+}_{n_1n_2r'}(p,q,t)=i\theta(r)\langle[\Phi_{n_1\downarrow}{}^{\dagger}(p+q,t)\Phi_{n_2\uparrow}(p,t),\sum_{k,k'}\Psi_{r'\uparrow}{}^{\dagger}(k+k')\Psi_{r'\downarrow}(k)]\rangle\ . \tag{C4}$$

It then follows that

$$\chi^{-+}_{rr'}(q,t)=\sum_p\sum_{n_1n_2}u_{n_1r}(p+q)u_{n_2r}(p)\chi^{-+}_{n_1n_2r'}(p,q,t)\ . \tag{C5}$$

The equations of motion for $\chi^{-+}_{m_1n_2r'}(p,q,t)$ are

$$i\partial_t\chi^{-+}_{m_1n_2r'}(p,q,t)=-\delta(t)\langle[\Phi_{n_1\downarrow}{}^{\dagger}(p+q,t)\Phi_{n_2\uparrow}(p,t),\sigma^+_{r'r'}(0,0)]\rangle$$
$$+i\theta(t)\langle[[\Phi_{n_1\downarrow}{}^{\dagger}(p+q,t)\Phi_{n_2\uparrow}(p,t),H_{\mathrm{eff}}],\sigma^+_{r'r'}(0,0)]]\rangle \tag{C6}$$

It can be seen from analyzing $[\Phi_{n_1\downarrow}{}^{\dagger}(p+q,t)\Phi_{n_2\uparrow}(p,t),H_{\mathrm{eff}}]$ that, for the contractions which are unrelated to self-energy corrections, momentum conservation requires momentum $\mathbf{K}$ in $J_H(\mathbf{K})$ to be always equal to $\pm\mathbf{q}$, the external

momentum. This variable can be removed from the internal summation. Consequently the expression for the RPA susceptibility can be written in "closed form." It should be stressed that this resummation depends on the detailed form of the vertex function given in Eq. (C2). This point can also be understood diagrammatically. For the *spin* susceptibility, the vertex Γ generates only a "bubble" series, and the momentum associated with the interaction line is always equal to $\pm q$.

Neglecting the self-energy corrections, and inserting the resulting expression for $[\Phi_{n_1\downarrow}^{\dagger}(p+q,t)\Phi_{n_2\uparrow}(p,t),H_{\text{eff}}]$ into Eq. (C6), we find that

$$\chi^{-+}_{n_1n_2r'}(p,q,\omega)=\chi^{0-+}_{n_1n_2}(p,q,\omega)u_{n_1r'}(p+q)u_{n_2r'}(p) + J_H(q)\chi^{0-+}_{n_1n_2}(p,q,\omega)u_{n_1d}(p+q)u_{n_2d}(p)\sum_{km_1m_2}u_{dm_1}(k+q)u_{dm_2}(k)\chi^{-+}_{m_1m_2r'}(k,q,\omega)\ , \tag{C7}$$

where

$$\chi^{0-+}_{n_1n_2}(p,q,\omega)=\frac{f_{n_1\downarrow}(p)-f_{n_2\uparrow}(p+q)}{\omega-[E_{n_1}(p)-E_{n_2}(p+q)]+i\eta}\ . \tag{C8}$$

The above analysis leads to

$$\sum_{km_1m_2}u_{dm_1}(k+q)u_{dm_2}(k)\chi^{-+}_{m_1m_2r'}(k,q,\omega)=\frac{\chi^{0-+}_{dr'}(q,\omega)}{1+J_H(q)\chi^{0-+}_{dd}(q,\omega)}\ . \tag{C9}$$

Combining Eqs. (C5), (C7), and (C9) we finally arrive at the RPA form

$$\chi^{-+}_{rr'}=\chi^{0-+}_{rr'}(q,\omega)+\frac{\chi^{0-+}_{rd}(q,\omega)[-J_H(q)]\chi^{0-+}_{dr'}(q,\omega)}{1-[-J_H(q)]\chi^{0-+}_{dd}(q,\omega)}\ . \tag{C10}$$

---

*Present address: Serin Physics Laboratory, Rutgers University, Piscataway, NJ 08855-0849.

†Present address: Physics Department, University of Illinois, Urbana-Champaign, IL 61801.

[1]S. Chakravarty, B. Halperin, and D. Nelson, Phys. Rev. B **39**, 2344 (1989); A. Auerbach and D. P. Arovas, Phys. Rev. Lett. **61**, 617 (1988); H. Q. Ding and M. S. Makivic, *ibid.* **64**, 1449 (1990).

[2]See, for example, B. Barbara, A. F. Khoder, M. Couach, C. Ayache, E. Bonjour, and R. Calemczuk, Physica C **153-155**, 912 (1988).

[3]C.G. Olson, R. Liu, D. W. Lynch, R. S. List, A. J. Arko, B. W. Veal, Y. C. Change, P. Z. Jiang, and A. P. Paulikas, Phys. Rev. B **42**, 381 (1990), and references therein.

[4]D. R. Harshman, G. Aeppli, G. P. Espinosa, A. S. Cooper, J. P. Remeika, E. J. Ansaldo, T. Riseman, D. L. Williams, D. R. Noakes, B. Ellman, and T. F. Rosenbaum, Phys. Rev. B **38**, 852 (1988); J. M. Tranquada, S. M. Heald, A. R. Moodenbaugh, M. Suenaga, *ibid.* **35**, 7187 (1987); G. Shirane, R. J. Birgeneau, Y.Endoh, P. Gehring, M. A. Kastner, K. Kitazawa, H. Kojima, I. Tanaka, T. R. Thurston, and K. Kitazawa, Phys. Rev. Lett. **63**, 330 (1989).

[5]C. H. Pennington, D. J. Durand, C. P. Slichter, J. P. Rice, E. D. Bukowski, and D. M. Ginsberg, Phys. Rev. B **39**, 2902 (1989).

[6]For calculations primarily appropriate to the La-Sr-Cu-O family, see J. P. Lu, Q. Si, J. H. Kim, and K. Levin, Phys. Rev. Lett. **65**, 2466 (1990); see also, Lu *et al.*, Physica C **179**, 191 (1991). For calculations primarily appropriate to the Y-Ba-Cu-O family, see Y. Zha, Q. Si, and K. Levin (unpublished).

[7]For a general review, see K. Levin *et al.*, Physica C **175**, 449 (1991); Ju H. Kim, K. Levin, and A. Auerbach, Phys. Rev. B **39**, 11 633 (1989).

[8]E. Arrigoni, G. Strinati, and C. Castellani, Phys. Rev. B **41**, 4838 (1990); J. F. Annett, R. M. Martin, A. K. McMahan, and S. Satpathy, *ibid.* **40**, 2620 (1989).

[9]D. M. Newns, P. Pattnaik, M. Rasolt, and D. A. Papaconstantopolulos, Phys. Rev. B **38**, 7033 (1988); D. M. Newns and P. C. Pattnaik, in *Strong Correlation and Superconductivity,* edited by H. Fukuyama, S. Maekawa, and A.P. Malozemoff (Springer-Verlag, Heidelberg, 1989).

[10]G. Kotliar, P. A. Lee, and N. Read, Physica C **153-155**, 538 (1988).

[11]A. Auerbach and K. Levin, Phys. Rev. Lett. **57**, 877 (1986); A. J. Millis and P. A. Lee, Phys. Rev. B **35**, 3394 (1987).

[12]A. Houghton, N. Read, and H. Won, Phys. Rev. B **37**, 3782 (1988).

[13]See, for example, A. K. McMahan, R. M. Martin, and S. Satpathy, Phys. Rev. B **38**, 6650 (1988).

[14]N. Read and D. M. Newns, J. Phys. C **16**, 3273 (1983).

[15]A. Aharony, R. J. Birgeneau, A. Coniglio, M. A. Kastner, and H. E. Stanley, Phys. Rev. Lett. **60**, 1330 (1988).

[16]L. P. Gor'kov and A. V. Sokol, Physica C **159**, 329 (1989).

[17]F.C. Zhang and T. M. Rice, Phys. Rev. B **37**, 3759 (1988). Implicit in our Fermi-liquid picture is the assumption that the rigid Zhang-Rice singlets do not persist for a finite hole concentration and physical values of the oxygen bandwidth.

[18]J. P. Lu and Q. Si, Phys. Rev. B **42**, 950 (1990).

[19]On the basis of previous work which describes coherent hole motion [see, for example, C. L. Kane, P. A. Lee, and N. Read, Phys. Rev. B **39**, 6880 (1989)], it may be argued that in the very dilute limit, an analysis similar to that presented here in the Fermi-liquid regime may be used where the characteristic interband separation Δ is replaced by the superexchange interaction J_S. Thus for $D \gg J_S$, large frequency fluctuations are still the dominant contribution to the exchange

interaction integrals. In this sense, then, the present picture may be more precise than a strict interpolation scheme when localized phases are present.

[20]S. Doniach, Phys. Rev. B **35**, 1814 (1987).

[21]A. J. Millis, H. Monien, and D. Pines, Phys. Rev. B **42**, 167 (1990); N. Bulut, D. Hone, D. J. Scalapino, and N.E. Bickers, Phys. Rev. Lett. **64**, 2723 (1990).

[22]N. Andrei and P. Coleman, Phys. Rev. Lett. **62**, 595 (1989).

[23]At large values of δ our mean-field phase diagram is equivalent to results derived in C. LaCroix and M. Cyrot, Phys. Rev. B **20**, 1969 (1979) for heavy-fermion systems.

[24]C. Jayaprakash, H.R. Krishnamurthy, and Sanjoy Sarker, Phys. Rev. B **40**, 2610 (1989).

[25]D. C. Johnston, Phys. Rev. Lett. **62**, 957 (1989).

[26]J. M. Tranquada, W. J. L. Buyers, H. Chou, T.E. Mason, M. Sato, S. Shamoto, and G. Shirane, Phys. Rev. Lett. **64**, 800 (1990).

[27]K. B. Lyons, P. A. Fleury, L. F. Schneemeyer, and J.V. Waszczak, Phys. Rev. Lett. **60**, 732 (1988).

[28]Q. Si, J.H. Kim, J. P. Lu, and K. Levin, Phys. Rev. B **42**, 1033 (1990).

[29]P. A. Wolff, Phys. Rev. **120**, 814 (1960); T. Izuyama, D.-J. Kim, and R. Kubo, J. Phys. Soc. (Jpn) **18**, 1025 (1963).

[30]S. Doniach and E. H. Sondheimer, *Green's Functions for Solid State Physics* (Benjamin/Cummings, Massachusetts, 1974).

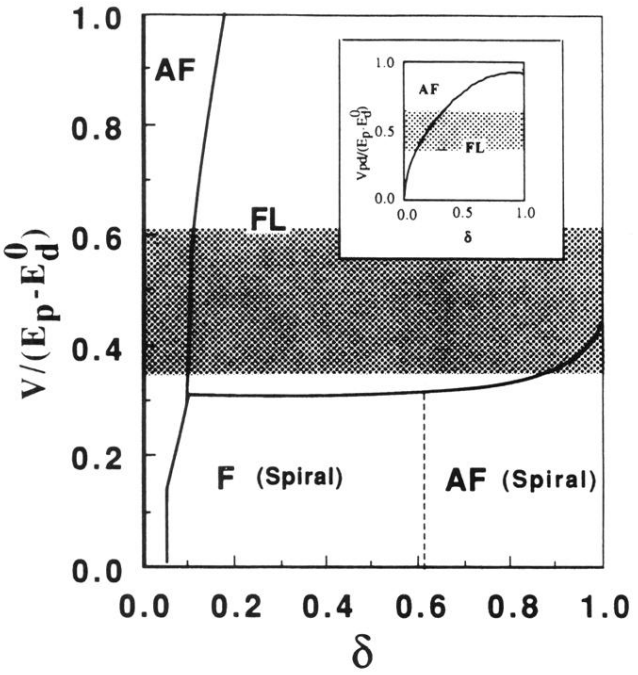

FIG. 2. The mean-field phase diagram for physically large conduction band width. In the inset is plotted the analogous phase diagram for zero bandwidth. F, AF, FL stand for ferromagnetic, antiferromagnetic, and Fermi-liquid phases, respectively. The shaded region corresponds to the physical parameter region (see text). The F and AF phases exhibit spiral order, as also discussed in the text.